

# eScholarship@UMassChan

**The C-terminal domain of SEC-10 is fundamental for excyst function, Spitzenkörper organization and cell morphogenesis in *Neurospora crassa* [preprint]**

Item Type	Preprint
Authors	Figuroa-Meléndez, Alfredo;Martínez-Núñez, Leonora;Rico-Ramírez, Adriana M.;Martínez-Andrade, Juan M.;Munson, Mary;Riquelme, Meritxell
Citation	<p>bioRxiv 2022.01.14.475644; doi: <a href="https://doi.org/10.1101/2022.01.14.475644">https://doi.org/10.1101/2022.01.14.475644</a> . <a href="https://doi.org/10.1101/2022.01.14.475644" target="_blank">Link to preprint on bioRxiv</a>.</p>
DOI	<a href="https://doi.org/10.1101/2022.01.14.475644">10.1101/2022.01.14.475644</a>
Rights	The copyright holder for this preprint is the author/funder, who has granted bioRxiv a license to display the preprint in perpetuity. It is made available under a <a href="http://creativecommons.org/licenses/by-nc-nd/4.0/">CC-BY-NC-ND 4.0 International license</a> .
Download date	2026-05-16 02:37:20
Item License	<a href="http://creativecommons.org/licenses/by-nc-nd/4.0/">http://creativecommons.org/licenses/by-nc-nd/4.0/</a>
Link to Item	<a href="https://hdl.handle.net/20.500.14038/30746">https://hdl.handle.net/20.500.14038/30746</a>

1 **The C-terminal domain of SEC-10 is fundamental for exocyst function, Spitzenkörper organization and**  
2 **cell morphogenesis in *Neurospora crassa*.**

3 **Alfredo Figueroa-Meléndez<sup>1</sup>, Leonora Martínez-Núñez<sup>2</sup>, Adriana M. Rico-Ramírez<sup>1,3</sup>, Juan M. Martínez-**  
4 **Andrade<sup>1</sup>, Mary Munson<sup>2</sup> and Meritxell Riquelme<sup>1</sup>**

5 <sup>1</sup>Department of Microbiology, Centro de Investigación Científica y de Educación Superior de Ensenada  
6 (CICESE), Ensenada, BC 22860, Mexico

7 <sup>2</sup>Department of Biochemistry and Molecular Pharmacology, University of Massachusetts Medical School,  
8 Worcester, Massachusetts 01605

9 <sup>3</sup>Department of Plant and Microbial Biology, University of California, Berkeley, California 94720, USA

10 **Keywords: Exocyst, *Neurospora crassa*, mass spectrometry, SEC-10, Spitzenkörper**

11 **Abstract**

12 The exocyst is a conserved multimeric complex that participates in the final steps of the secretion of  
13 vesicles. In the filamentous fungus *Neurospora crassa*, the exocyst is crucial for polar growth,  
14 morphology, and the organization of the Spitzenkörper (Spk), the apical body where secretory vesicles  
15 accumulate before being delivered to the plasma membrane. In the highly polarized cells of *N. crassa*,  
16 the exocyst subunits SEC-3, SEC-5, SEC-6, SEC-8, and SEC-15 were previously found localized at the  
17 plasma membrane of the cells' apices, while EXO-70 and EXO-84 occupied the frontal outer layer of the  
18 Spk, occupied by vesicles. The localization of SEC-10 had remained so far elusive. In this work, SEC-10  
19 was tagged with the green fluorescent protein (GFP) either at its N- or C-terminus and found localized at  
20 the plasma membrane of growing hyphal tips, similar to what was previously observed for some exocyst  
21 subunits. While expression of an N-terminally tagged version of SEC-10 at its native locus was fully  
22 viable, expression of a C-terminally tagged version at its native locus resulted in severe hyphal growth  
23 and polarity defects. Additionally, a *sec-10* knockout mutant in a heterokaryotic state (with genetically  
24 different nuclei) was viable but showed a strongly aberrant phenotype, confirming that this subunit is  
25 essential to maintain hyphal morphogenesis. Transmission electron microscopy analysis revealed the  
26 lack of a Spk in the SEC-10-GFP strain, suggesting a critical role of the exocyst in the vesicular  
27 organization at the Spk. Mass spectrometry analysis revealed fewer peptides of exocyst subunits  
28 interacting with SEC-10-GFP than with GFP-SEC-10, suggesting an essential role of the C-terminus of SEC-  
29 10 in exocyst assembly and/or stability. Altogether, our data suggest that an unobstructed C-terminus of

30 SEC-10 is indispensable for the exocyst complex function and that a GFP tag could be blocking important  
31 subunit-subunit interactions.

32

### 33 **Introduction**

34 Filamentous fungi are excellent model organisms to study polarized growth. Fungal hyphae extend by a  
35 sustained polarized process that involves the apical exocytosis of secretory vesicles that fuse with the  
36 plasma membrane (PM), allowing the secretory vesicles to deliver their content to the extracellular  
37 space (Riquelme et al., 2011; Rizzoli and Jahn, 2007). Exocytosis is fundamental for many cellular  
38 activities, including neurotransmitter release at the presynaptic terminal, vesicular transport to the  
39 basolateral membrane, and primary ciliogenesis in animal cells, expansion of root hair tips in plants, and  
40 hyphal tip growth in fungi, all of which involve polarized secretion of vesicles (Grindstaff et al., 1998;  
41 Kennedy and Ehlers, 2011; Lopez-Franco et al., 1994; Monshausen et al., 2008; Zuo et al., 2009). The  
42 interaction between a vesicle and a target membrane throughout the different steps of the secretory  
43 and endocytic pathways is mediated by multisubunit tethering complexes (MTCs) (Dubuke and Munson,  
44 2016). The exocyst complex is a highly conserved MTC within eukaryotes that was first identified in the  
45 budding yeast *Saccharomyces cerevisiae*. It consists of the proteins Sec3, Sec5, Sec6, Sec8, Sec10, Sec15,  
46 Exo70, and Exo84 (Guo et al., 1999; TerBush et al., 1996; TerBush and Novick, 1995). This complex has  
47 been linked to several diseases and exocyst mutants are associated with cell growth and developmental  
48 defects, as has been shown in mouse and *Drosophila* models (Friedrich et al., 1997; Martin-Urdiroz et  
49 al., 2016; Murthy et al., 2003; Murthy et al., 2005). Consistent with an essential role in fusion of  
50 secretory vesicles at exocytic sites, temperature sensitive mutants of exocyst subunits cause an  
51 accumulation of secretory vesicles in the cytoplasm (Novick, 1980).

52 The exocyst is proposed to mediate the tethering of post Golgi secretory vesicles to the PM and to  
53 promote the fusion of membranes via SNARE complexes (Heider and Munson, 2012; TerBush et al.,  
54 1996; Wu and Guo, 2015; Yue et al., 2017), but mechanistic details are lacking. A reconstruction of the  
55 3D architecture of the *S. cerevisiae* exocyst *in vivo* suggested that the subunits' N-terminal ends are  
56 oriented towards the center of the complex, except for Sec10, whose C-terminus is the one oriented  
57 toward the center (Picco et al., 2017). The near-atomic cryo-EM structure of the *S. cerevisiae* exocyst  
58 revealed that all exocyst subunits are rod-shaped (Lepore et al., 2018; Mei et al., 2018). The subunits  
59 contain long N-terminal (except for Sec3, where the region is centrally located) coiled regions called

60 CorEx (core of the exocyst) that assemble together to generate the framework of the complex in the  
61 form of two modules of four subunits each, which consist of subcomplex I (Sec3, Sec5, Sec6 and Sec8)  
62 and subcomplex II (Sec10, Sec15, Exo70 and Exo84) that pack against one another (Lepore et al., 2018;  
63 Mei et al., 2018).

64 In the filamentous fungus *Neurospora crassa*, a full exocyst with the eight subunits is required for  
65 maintaining polarized hyphal growth and for the orderly arrangement of large secretory vesicles  
66 (macrovesicles) at the Spitzenkörper (Spk) (Riquelme et al., 2014). Deletion of *sec-5* severely affected  
67 cell morphogenesis and the apical localization of macrovesicles in *N. crassa*. GFP tags were added at the  
68 3' end of the endogenous loci encoding the different exocyst subunits; the subunits SEC-5, SEC-6, SEC-8,  
69 and SEC-15 localized at the PM in *N. crassa* hyphal tips, whereas EXO-70 and EXO-84 localized at the  
70 frontal periphery of the Spk (Riquelme et al., 2014). SEC-3 was observed at both the PM and the Spk. In  
71 the *sec-5* mutant background, SEC-6-GFP and EXO-70-GFP were not localized at the hyphal apex,  
72 suggesting that SEC-6 and EXO-70 localization depends on SEC-5 (Riquelme et al., 2014).

73 Curiously, in previous studies, no viable transformed *N. crassa* strains could be recovered for the C-  
74 terminally GFP tagged SEC-10 subunit. Similar results were reported for the rice blast fungus  
75 *Magnaporthe oryzae*, where SEC-10 was the only subunit that could not be successfully tagged, which  
76 suggested that a tag at the C-terminus of SEC-10 could interfere with function in SEC-10 nearby  
77 subunits, or exocyst binding partners (Gupta et al., 2015). Further, *S. cerevisiae* cells overexpressing  
78 Sec10 $\Delta$ C, a protein lacking the C-terminal region, led to a block in exocytosis and accumulation of  
79 vesicles (Roth et al., 1998).

80 In this study, we endogenously tagged the SEC-10 exocyst subunit with GFP at either its N- or C-  
81 terminus, as well as produced mutants of *N. crassa* either lacking *sec-10* or harboring a truncated  
82 version of *sec-10*, to test the importance of the C-terminal region. We analyzed by SDS-PAGE and mass  
83 spectrometry the proteins recovered from pull downs of both the C-terminally tagged SEC-10 and the N-  
84 terminally tagged SEC-10. We found that deleting *sec-10* or tagging *sec-10* at the C-terminus had a  
85 similar detrimental effect on growth, whereas tagging *sec-10* at the N-terminus or eliminating 40 amino  
86 acids from the C-terminus of *sec-10* had no significant impact on growth rate. Our results suggest that  
87 the GFP tag at the C-terminus affects the stability of the complex by acting as a spatial impediment for  
88 the assembly of the exocyst subunits and could be destabilizing important protein-protein interactions  
89 within the complex.

## 90 **Materials and methods**

### 91 **Strains used or generated in this study**

92 The *N. crassa* strain FGSC9718 was used to tag SEC-10 with GFP and to delete the *sec-10* gene. All strains  
93 were cultured in Vogel's Minimal Medium (VMM; (Vogel, 1956) supplemented with 1.5% sucrose and  
94 incubated at 30 °C. To select putative transformants, VMM was supplemented with 0.05% fructose,  
95 0.05% glucose, 2% sorbose (FGS), and hygromycin B (Hyg, 300 µg/mL; Invitrogen, Carlsbad, CA). All *N.*  
96 *crassa* strains that were used or developed in this study are listed in Table 1.

### 97 ***In silico* analysis of SEC-10**

98 Functional and structural information about SEC-10 was analyzed using the UniProt protein  
99 identification code for *N. crassa* (Q7SD81\_NEURCR) on several different servers. Similar analyses were  
100 performed for SEC-10 orthologues found in *C. albicans*, *S. cerevisiae*, *A. nidulans* and *M. oryzae*. The  
101 different functional domains were identified using the UniProtKB database (<https://www.uniprot.org/>).  
102 The motifs contained in these sequences were identified using ScanProsite (<https://prosite.expasy.org>)  
103 and superfamily domains on the InterPro server (<http://www.ebi.ac.uk/interpro/>). The presence of  
104 predicted disordered domains in the subunits' structure was detected with the MobiDB server, which  
105 uses a consensus method that is optimized to find long intrinsically disordered protein (IDRs). MobiDB is  
106 integrated in InterProScan and its predictions are propagated to several EBI resources (PDBe, UniProt,  
107 InterPro). (<http://mobidb.bio.unipd.it/>).

### 108 **Tagging SEC-10 with GFP**

109 The SEC-10 protein was endogenously tagged at the C- or N-terminus using the Split-Marker gene  
110 replacement technique as previously described (Smith et al., 2011). The C-terminus was tagged by using  
111 constructs for homologous gene replacement based on pGFP::*hph*::loxP (Honda and Selker, 2009);  
112 GeneBank accession number FJ457011; Fig. S1A), whereas the N-terminus was tagged by using  
113 constructs based on pGFP::*hph*::loxP and pCCG::*N-GFP* (Honda and Selker, 2009); Fig. S1B). The  
114 replacement cassettes contained the selectable hygromycin resistance marker (*hph*) (Fig. S1B). The  
115 genomic regions of *sec-10* were amplified from genomic DNA of *N. crassa* N1 that was extracted with a  
116 DNeasy Plant Mini Kit (Qiagen, Valencia, CA) (Table 1). A total of 1 µg of DNA (500 ng of each DNA  
117 replacement cassette) was mixed with 1.25E8 macroconidia of the FGSC9718 strain and transferred to  
118 0.2 cm-gap sterile electroporation cuvettes (BIO-RAD® GenePulser Xcell™) for transformation by

119 electroporation (1500 V, 25  $\mu$ F, 600 Ohm) (Margolin et al., 1997)). Electroporated cells were plated in  
120 VMM-FGS agar containing a final concentration of 300  $\mu$ g/mL of hygromycin. SEC-10 was also tagged  
121 ectopically at the C-terminus by using a *his-3* targeting vector containing a *Pccg1::sec-10::gfp* cassette  
122 (VMRP-114; unpublished). The plasmid (1  $\mu$ g) linearized with *NdeI* and treated with Shrimp Alkaline  
123 Phosphatase was used to transform 1.25E8 macroconidia of the FGSC9717 histidine auxotrophic strain  
124 via electroporation. The genetic constructs and the fusions are shown in Supplementary figure 1.

### 125 **Laser scanning confocal microscopy cell preparations**

126 Conidia from a preserved stock were inoculated on VMM 1.5% agar plates and incubated overnight at  
127 30 °C. A small rectangular section of 1.5 cm x 2 cm was cut out from the plate with a sterile spatula. The  
128 face of the agar containing the mycelium was placed carefully over a cover slide (VWR VistaVision™  
129 Cover Glasses 16004-096, No. 1, 24 x 60 mm) and left at room temperature for 15 min. A small drop of  
130 immersion oil was placed over a 60X objective lens. The slide was loaded on the stage on an Olympus  
131 FluoView™ FV1000 laser scanning confocal microscope (LSCM). The images were acquired on a confocal  
132 LSM observation mode with a PLAPON 60X O NA:1.42 objective lens, a oneway XYT scan mode, and a  
133 scanning speed of 20 us/pixel. The region of interest was clipped with a rectangular tool of the  
134 FLUOVIEW FV1000 software version 4.0.2.9. To image GFP, a blue Argon-ion laser was used with an  
135 excitation wavelength of 488 nm and an emission wavelength of 510 nm. In the case of cells expressing  
136 the mCherry fluorescent protein (mChFP) or stained with FM4-64, a green Helium-Neon laser was used  
137 with an excitation wavelength of 543 nm and an emission wavelength of 612 nm. FM4-64 is a lipophilic  
138 stain that labels membranes inside the cell (Pogliano et al., 1999). Images of the colonies were taken to  
139 compare the phenotype and characteristics of the strains. The strains were incubated 24 h at 30 °C, and  
140 photographs of these colonies were taken (Nikon Digital Camera D33697, Nikon Corp., Japan). Each  
141 colony was observed under a stereomicroscope (Olympus Optical Co., Ltd. Model SZX-ILLB2-100) on  
142 different objective lenses.

### 143 **Transmission electron microscopy cell preparations**

144 Conidia of *N. crassa* strain expressing SEC-10-GFP were inoculated on sterile and deionized dialysis  
145 membranes overlaid on VMM 1.5% agar plates and grown at 27 °C for 48 h. Subsequently, 5x5 cm  
146 squares (n=80) containing growing hyphae were cut, let recover for 30 min, and cryo-fixed by rapidly  
147 immersing them in liquid propane cooled to -186 °C with liquid nitrogen as previously described (Dunn  
148 and Wobbe, 1993). The samples were transferred to 2% osmium tetroxide and 0.05% uranyl acetate in

149 acetone at -80°C for 72 h. After that, they were washed three times in 100% anhydrous acetone,  
150 infiltrated in Spurr resin, and embedded in Teflon coated glass slides to be polymerized at 60 °C for 24 h.  
151 For semi-quantitative analysis, hyphae (n=10) were selected randomly from different regions of the  
152 samples to obtain ultrathin medial sections (70 nm). All the samples were observed using a Hitachi  
153 H7500 transmission electron microscope to 80 kV with a 16-megapixel Gatan CCD digital camera.

#### 154 **Producing *sec-10* mutant strains**

155 An *N. crassa sec-10* knock-out mutant strain was obtained from the Fungal Genetic Stock Center  
156 (FGSC11723) and tested to confirm the gene's deletion. Genomic DNA was extracted and tested via PCR  
157 with oligonucleotides that flank the *sec-10* open reading frame (ORF). Since an amplicon of the  
158 corresponding *sec-10* ORF length was obtained from the presumable mutant, confirming a  
159 heterokaryotic stage, recovery of a homokaryotic strain was attempted by genetic crossing with the  
160 wild-type strain N150 (FGSC9013). Heterokaryosis refers to the presence of genetically distinct nuclei  
161 within the same cell, and homokaryosis refers to the presence of genetically identical nuclei within the  
162 cell (Strom and Bushley, 2016). However, deletion of the *sec-10* ORF could not be confirmed through  
163 PCR. These results led us to produce our own *sec-10* knock-out mutant strain by using the Split-Marker  
164 gene replacement technique (Fig. S1C). Genomic DNA from *N. crassa* Wild Type FGSC988 was extracted  
165 with a DNeasy Plant Mini Kit (Qiagen, Valencia, CA). The plasmid pGFP::*hph*::*loxP* was purified with a  
166 Qiagen plasmid isolation kit. The knock-out constructs were produced using genomic DNA and  
167 oligonucleotides with *hph* gene sequence overhangs (Table 2). The 1 kb of the 5' untranslated region  
168 (UTR) was amplified with forward primer 720 and reverse primer 721 that flank the *hph* gene. The 1 kb  
169 of the 3' UTR was amplified with a forward primer that contains an overhang that overlaps with the 5'  
170 region of the *hph* gene and a reverse primer that overlaps with the 3' end of 3' UTR region. These two  
171 constructs flank the ORF region of *sec-10*, and upon homologous recombination the *hph* gene replaces  
172 *sec-10* (Fig. S1C). A deletion mutant named *sec-10*<sup>840-880del</sup> was also created to test the effects of deleting  
173 the C-terminal disordered domain, which consists of 40 amino acids by eliminating the last 120  
174 nucleotides of the *sec-10* ORF (Fig. S1D), which corresponds to a short C-terminus disordered domain.  
175 The reverse oligonucleotide included an overhang that overlaps with the *hph* gene and excluded the 120  
176 nucleotides by moving the stop codon 120 nucleotides upstream (Fig. S1D). *N. crassa* strain FGSC9718  
177 macroconidia were transformed with the DNA constructs by electroporation. Transformants were  
178 plated on VMM agar solidified with hygromycin at a final concentration of 300 µg/mL.

#### 179 **SEC-10-GFP and GFP-SEC-10 pull-downs with Lag 94-15 for mass spectrometry analysis**

180 Strains expressing cytoplasmic GFP, N-terminal tagged SEC-10, and C-terminal tagged SEC-10 were  
181 grown on VMM plates. The mycelium was scraped from the agar and transferred to Erlenmeyer flasks  
182 with liquid VMM for incubation at 200 rpm, 30 °C (INFORS Multitron CH-4103). After vacuum filtration,  
183 the recovered biomass was pulverized in a planetary ball mill (Retsch PM100) under liquid nitrogen  
184 conditions and stored at -80 °C until use. 150 mg of frozen powder were added to a 1.5 mL  
185 microcentrifuge tube and resuspended in 650 µL lysis buffer (20 mM Tris pH 8.5, 150 mM KCl, 0.1%  
186 Tween 20 and 1x cOmplete Mini EDTA-free protease inhibitor solution; Roche Life Science). The  
187 suspension was spun at 14,000 g for 10 min at 4°C. The supernatant was incubated with 15 µL of M270  
188 magnetic amine Dynabeads covalently bound to anti-GFP LaG94-15 nanobody (Fridy et al., 2014) at 4 °C  
189 for 1 h, nutating. The beads were washed three times with lysis buffer and resuspended in 25 µL of lysis  
190 buffer and 5 µL of 5X SDS-PAGE buffer. The samples were boiled at 95 °C for 5 min and used to run an  
191 SDS-PAGE (Novex™ WedgeWell™ 4 to 20%, Tris-Glycine, 1.0 mm, Mini Protein Gel) followed by 1X  
192 Krypton™ fluorescent staining (Thermo Fischer Scientific). Proteins were visualized on a Typhoon FLA  
193 9000 (Ex/Em = 532/580 nm).

#### 194 **Mass spectrometry sample preparation**

195 For mass spectrometry analysis, the pull-down was scaled up to 750 mg of pulverized mycelium  
196 resuspended in 1 mL of lysis buffer. The sample was run a small distance into the gel by electrophoresis  
197 so that the gel sample would contain the exocyst complex binding partners. The gel was stained with  
198 Coomassie solution and cut into 1x1 mm pieces per sample, which were kept in 1.5 mL tubes with milliQ  
199 water until mass spectrometry analysis. The water was discarded, and the gel pieces were incubated in  
200 10 mM 1,4 dithiothreitol (DTT) in ammonium bicarbonate solution at 50 °C to reduce the disulfide  
201 bands, followed by iodoacetamide (IAA) alkylation at room temperature. The remaining DTT and IAA  
202 were removed, followed by three wash steps with water, 50 mM ammonium bicarbonate: acetonitrile  
203 (50:50), and 100% acetonitrile. The acetonitrile was discarded, and the samples were dried in a Speed  
204 Vac lyophilizer. After complete drying, trypsin enzyme and proteaseMAX surfactant in ammonium  
205 bicarbonate solution were placed in the tubes, and digestion was performed for 18 hours at 37 °C. Then  
206 the samples were spun down, the supernatant was removed and placed in a new tube, and gel pieces  
207 were further dehydrated in a solution of acetonitrile: 1% formic acid in water (80:20) while. The samples  
208 were spun down, and the resulted supernatant was combined with the previous one, and the peptide  
209 mixture was dried down in a Speed Vac lyophilizer. The obtained peptide pellets were resolubilized in  
210 5% acetonitrile with 0.1% formic acid in water to prepare the samples for analysis.

## 211 **Liquid chromatography and mass chromatography analysis**

212 The liquid chromatography tandem mass spectrometry (LC-MS/MS) analysis was performed on a Waters  
213 nanoAcquity UPLC (Waters, Milford, MA) and a Q Exactive hybrid quadrupole-Orbitrap mass  
214 spectrometer (Thermo Fisher Scientific Inc., Waltham, MA).

215 The peptides were trapped (4 mins) in an in-house packed pre-column (C18, 200A, 5 $\mu$ m, 2cm), then the  
216 peptide separation started at 5% organic phase B (acetonitrile with 0.1 % formic acid) and 95% aqueous  
217 phase A (water with 0.1 % formic acid). The gradient was carried on to 35% B over 90 mins, on an in-  
218 house packed analytical column (C18, 100A, 3  $\mu$ m, 25 cm), followed by 90% B for 10 mins wash, and 5%  
219 B for 15 mins (re-equilibration). The MS data acquisition was performed in positive electrospray  
220 ionization mode (ESI+), within the mass range of 300-1750 Da for MS1, with the orbitrap resolution of  
221 70,000 at m/z 200. The maximum injection time and the AGC target were set to 30 ms and 1e6,  
222 respectively. Data Dependent Acquisition (DDA) MS/MS was applied on the top 10 precursor ions within  
223 a 1.6 Da isolation window, with the resolution of 17500 at m/z 200. The maximum injection time and  
224 the AGC target for the MS/MS were set to 110 ms and 1e5, respectively. The normalized collision energy  
225 was set to 27 V for fragmentation.

## 226 **Mass spectrometry data processing**

227 The acquired MS raw data was imported to Thermo Proteome Discoverer (PD) 2.1.1.21 (Thermo Fisher  
228 Scientific Inc.) software for processing. The data was searched against UniProt database using Mascot  
229 Server 2.6.2 (Matrix Science Ltd) in PD. Two maximum missed cleavages were considered for trypsin  
230 digestion. The peptide modifications were set to carbamidomethyl of cysteine as fixed modification, and  
231 three variable modifications of methionine oxidation, N-terminal acetylation, and N-terminal glutamine  
232 to pyroglutamate. The error tolerance was specified as 10 ppm for the monoisotopic mass of the  
233 precursor and 0.05 Da for the fragment mass. The data was further processed by Scaffold 4.10.0  
234 (Proteome Software Inc.) to validate peptide and protein identification. Scaffold applied a 1% false  
235 discovery rate (FDR) for peptide identification based on the peptide Prophet algorithm (Keller et al.,  
236 2002). A minimum number of 2 peptides was considered as the threshold for protein identification with  
237 99% probability, applied by Scaffold, using protein Prophet algorithm (Nesvizhskii et al., 2003).

238

239

## 240 Results

### 241 The exocyst subunit SEC-10 localizes at the plasma membrane in hyphal tips

242 *N. crassa* SEC-10 orthologues in *Saccharomyces cerevisiae*, *Magnaporthe oryzae*, *Aspergillus nidulans*,  
243 and *Candida albicans* share a similar length, ranging from 785 to 880 amino acids. All SEC-10  
244 orthologues contain a predicted coiled-coil domain or domains, which are ~100 amino acids  
245 downstream from the N terminus (Fig. 1). Previously, SEC-10 was the only exocyst subunit that could not  
246 be successfully tagged endogenously at its C-terminus in *N. crassa* (Riquelme et al., 2014). In this study,  
247 we successfully obtained an *N. crassa* strain that expressed SEC-10 tagged with GFP. We created strains  
248 in which SEC-10 was both C-terminally (SEC-10-GFP) and N-terminally (GFP-SEC-10) tagged with GFP at  
249 its native locus, under the control of the native promoter (Fig. 2A), and also C-terminally tagged at the  
250 *his-3* locus under the control of the *ccg-1* promoter (pCCG-1-SEC-10-GFP; Fig. 2B). In all three cases, the  
251 resulting GFP-tagged SEC-10 protein localized at the apical PM (Fig. 2), similar to the localization  
252 previously described for the exocyst subunits SEC-5, SEC-6, SEC-8, and SEC-15 (Riquelme et al., 2014).  
253 Localization of GFP-SEC-10 fluorescence was similar to localization of SEC-10-GFP. Neither SEC-10-GFP  
254 nor GFP-SEC-10 showed co-localization with the Spk at the tip, as stained in live cells with FM4-64 (Fig.  
255 2C, E). In *N. crassa*, we can produce both homokaryon strains, which contain genetically identical nuclei,  
256 and heterokaryons, which contains two genetically different nuclei. We found that the homokaryon  
257 strain expressing SEC-10-GFP had irregular cell shapes, a barely visible Spk and a clear problem with  
258 maintaining growth (Fig. 2D).

### 259 GFP tagging of SEC-10 at the C-terminus caused growth defects and hyphal deformities

260 We compared the growth rates and cellular phenotypes of the endogenously tagged SEC-10-GFP  
261 heterokaryon, SEC-10-GFP homokaryon, GFP-SEC-10 homokaryon, and wild type 9718 strains. The  
262 corresponding genetic constructs introduced in each strain are shown in Fig. 6A. Growth defects and cell  
263 deformities were detected in the SEC-10-GFP homokaryon strain (Supplementary video 1) and to a  
264 lesser degree in the SEC-10-GFP heterokaryon strain. Differential interference contrast (DIC) microscopy  
265 and Laser scanning confocal microscopy (LSCM) revealed that the homokaryon strain SEC-10-GFP had a  
266 dispersed accumulation of FM4-64 at swollen hyphal tips (Fig. 3A), and a larger number of septa,  
267 resulting in unusually shorter compartments (Fig. 3B;  $26 \pm 0.8 \mu\text{m}$ , N=15) when compared to the wild-  
268 type strain (Fig 3C;  $159 \pm 10.2 \mu\text{m}$ , N=15). After 24 h of growth, the wild type, and the C-terminal SEC-10  
269 tagged strains showed clear differences in colony growth (Fig. 4). The wild-type strain covered almost

270 the entire agar surface of the Petri dish, whereas the SEC-10-GFP heterokaryon had only begun to  
271 colonize the surface, and in the homokaryotic state, the SEC-10-GFP strain had not yet developed. It was  
272 only after 7 days of growth when the SEC-10-GFP heterokaryon had fully colonized the surface. The  
273 homokaryon colony did not grow any further along the medium but began growing aerially (Fig. 4A).  
274 Stereomicrographs of these strains highlighted how compact the mycelium of the SEC-10-GFP  
275 homokaryon strain was when compared to the other strains (Fig. 4B). DIC microscopy revealed irregular  
276 cell shapes in all observed hyphae in both the SEC-10-GFP homokaryon and heterokaryon strains,  
277 although more so in the homokaryon (Fig. 4C; Fig. 6B). Notably, the hyphae of the SEC-10-GFP  
278 homokaryon strain displayed a larger hyphal diameter ( $11.8 \pm 0.7 \mu\text{m}$ ,  $N=25$ ) than the wild-type strain  
279 (Fig. 4C;  $8.46 \pm 0.7 \mu\text{m}$ ,  $N=25$ ) and the GFP-SEC-10 homokaryon strain ( $7.6 \pm 0.6 \mu\text{m}$ ,  $N=25$ ). Another  
280 characteristic of this strain was how the hyphae change direction momentarily, with a concomitant loss  
281 of the Spk localization (Fig. 5.; Supplementary video 2).

## 282 ***sec-10* is an essential gene required for cell growth and morphogenesis**

283 We next examined the phenotype of strains in which *sec-10* was deleted or truncated. The  $\Delta sec-10$   
284 mutant could not be obtained in a homokaryotic state by either microconidia production or genetic  
285 crossing, indicating that it is essential. However, the heterokaryon was viable but with delayed growth  
286 and almost a complete lack of conidia production; this mutant strain had a 99% reduction in  
287 macroconidia production, and 95% of the conidia produced were microconidia. In contrast, strain *sec-*  
288  $10^{840-880\text{del}}$ , a mutant with a C-terminally truncated SEC-10 protein, had no phenotypic or growth defects  
289 (Fig. 6B). Upon comparing the growth rate of the strains 9718 ( $2.8 \pm 0.29 \mu\text{m}$ ,  $N=16$ ), SEC-10-GFP  
290 heterokaryon ( $0.76 \pm 0.39 \mu\text{m}$ ,  $N=16$ ) and homokaryon ( $0.16 \pm 0.01 \mu\text{m}$ ,  $N=16$ ), GFP-SEC-10  
291 homokaryon ( $2.4 \pm 0.45 \mu\text{m}$ ,  $N=16$ ),  $\Delta sec-10$  heterokaryon ( $0.9 \pm 0.29 \mu\text{m}$ ,  $N=16$ ), and *sec-10*<sup>840-880del</sup>  
292 homokaryon ( $2.5 \pm 0.37 \mu\text{m}$ ,  $N=16$ ) (Fig. 6B), it was revealed that the growth rates of the C-terminal  
293 tagged SEC-10 homokaryon strain and the  $\Delta sec-10$  heterokaryon mutant strain were significantly  
294 reduced. In contrast, the N-terminal tagged SEC-10 strain did not show a significantly different growth  
295 rate than the wild-type strain. Together, our finding that the SEC-10-GFP homokaryon strain had an 83%  
296 growth rate reduction, as well as morphologic and cell polarity defects, indicates that the GFP tag at the  
297 C-terminus of SEC-10 perturbs exocyst function.

298

299 The genetic constructs that were used for electroporation are shown in Figure 6A, including the *sec-10*  
300 mutants  $\Delta sec-10$  and *sec-10*<sup>840\_880del</sup>. Growth and Spk morphology of all the SEC-10 tagged strains and  
301 *sec-10* mutants were analyzed. Both the  $\Delta sec-10$  and SEC-10-GFP homokaryon strains had poor colony  
302 development, unrecognizable Spk observed by FM4-64 staining LSCM analysis, swollen or bifurcated  
303 hyphal tips as revealed by DIC microscopy, and lower growth rate when compared to the wild-type  
304 strain. The GFP-SEC-10 protein localized at the hyphal tips much like the C-terminally tagged SEC-10 (Fig.  
305 2) and did not have any hyphal morphology defects or a decrease in growth rate (Fig. 6B; Supplementary  
306 video 3). We used transmission electron microscopy (TEM) analysis to examine the cells in greater  
307 detail. Representative TEM micrographs of medial sections confirmed the lack of an organized Spk in  
308 hyphal tips of the SEC-10-GFP homokaryon strain (Fig. 7). All hyphal tips had large amounts of  
309 macrovesicles dispersed in the dome region (Fig. 7 A, B), contrary to the organization seen in previous  
310 reports for the wild-type strain, where macrovesicles concentrate primarily in the outer layer of the Spk  
311 surrounding a core of microvesicles (Riquelme et al., 2014; Verdin et al., 2009). Interestingly, in few  
312 hyphae, a Spk core remained visible (Fig. 7B), whereas other hyphae did not appear to have a defined  
313 Spk core as seen in Fig. 7C.1-C.2.

#### 314 **SEC-10 co-localizes partially with Spk macrovesicles**

315 The Spk in *N. crassa* has a an inner core of microvesicles that contain chitin synthases (CHS) and an outer  
316 layer of macrovesicles that contain glucan synthase (GS) (Sánchez-León et al., 2011; Verdin et al., 2009).  
317 In a previous study, the subunits SEC-5, SEC-6, SEC-8, and SEC-15 were shown to localize at the PM of  
318 hyphal tips, whereas EXO-70 and EXO-84 localized at the frontal macrovesicular layer of the Spk  
319 (Riquelme et al., 2014). SEC-3 was the only subunit that was shown to be present in both locations. To  
320 explore whether SEC-10 associates with macro and/or microvesicles, the SEC-10-GFP protein was co-  
321 expressed with macro and microvesicle reporters tagged with mCherry fluorescent protein (mChFP). For  
322 this, SEC-10 was tagged at the C-terminus with GFP and expressed under the control of *Pccg-1* at the *his-*  
323 *3* locus. As the *sec-10* native locus was unaltered by GFP tagging, the resulting strain did not show any  
324 apparent growth defect or affected phenotype. This strain was fused with the strain that expresses CHS-  
325 1-mChFP to serve as a reporter for microvesicles, and another strain that expresses GS-1-mChFP as a  
326 reporter for macrovesicles. LSCM of the strain expressing SEC-10-GFP and CHS-1-mChFP revealed that  
327 SEC-10-GFP did not co-localize with the microvesicles localized at the Spk core (Fig. 8A). In contrast, in  
328 the strain expressing GS-1-mChFP and SEC-10-GFP, the SEC-10 protein partially co-localized with  
329 macrovesicles on the frontal outer layer of the Spk (Fig. 8B).

330

331 **The C-terminus of SEC-10 is important for the interactions with the exocyst subunits**

332 We used pull-down experiments, with anti-GFP nanobody-coupled beads, to examine the assembly and  
333 stability of the exocyst complex. SDS-PAGE and Krypton™ staining of the putative interacting proteins  
334 purified from the N-terminally and C-terminally tagged SEC-10 strains, indicated that the C-terminal tag  
335 severely disrupts the assembly of the exocyst complex. When the C-terminally tagged SEC-10 was pulled  
336 down, apparently only one exocyst subunit band was visibly detected in the gel. In contrast, in the N-  
337 terminally tagged SEC-10 strain, eight bands could be identified, which corresponded to each subunit of  
338 the exocyst complex in *N. crassa*, based on their molecular weight (Fig. 9A).

339 LC-MS/MS analyses of the pull-downs revealed that the C-terminally tagged SEC-10 had a substantially  
340 lower number of bound proteins present when compared to the pull-down from the N-terminal tagged  
341 strain. Mass spectrometry analysis of these two samples revealed a total of 258 proteins: 231 proteins in  
342 the N-terminally tagged SEC-10 sample, and 107 proteins in the C-terminally tagged SEC-10 sample, with  
343 80 proteins shared by both samples (data not shown). A cutoff of 14 hits or lower was used on the data,  
344 and the gene identities were categorized by Gene Ontology (GO) terms (Fig. S3). After the cutoff, only 26  
345 unique proteins remained for the N-terminally tagged sample and 9 proteins for the C-terminally tagged  
346 sample, with only 7 shared proteins that corresponded to the exocyst components (Fig. 9B). Regarding  
347 the exocyst subunits, the data showed that both samples shared seven exocyst subunits in common, but  
348 SEC-3 was excluded by the cutoff from the C-terminally tagged sample. Consistent with the gel in Figure  
349 9A, the C-terminally tagged SEC-10 sample had fewer detected peptides for every exocyst component,  
350 suggesting that the GFP tag at the C-terminus leads to weakened affinity of SEC-10 for the rest of the  
351 complex. The least abundant subunits, compared to the N-terminally tagged data set, identified in the C-  
352 terminally tagged SEC-10 sample were SEC-3, SEC-5, SEC-6, and SEC-8, which represented only around  
353 12-20% of the total amount of each subunit detected in the N-terminally tagged SEC-10 sample. In  
354 contrast, SEC-15, EXO-70, and EXO-84 were detected in the C-terminally tagged sample at 28-39% of the  
355 subunits detected in the N-terminally tagged sample (Fig. 9C). The number of single peptides for the GFP  
356 protein and Lag-94-15 nanobody protein were equally abundant in both samples, which served as  
357 internal controls.

358

359

## 360 Discussion

361 Our results demonstrate that tagging of the C-terminal end of SEC-10 disrupted exocyst function and  
362 complex stability. This disruption led to aberrant phenotypes observed in SEC-10-GFP homokaryon  
363 strains (Fig 6B). Even as a heterokaryon, the SEC-10-GFP strain showed slower growth and wider cells  
364 when compared to the wild type. The fact that the SEC-10-GFP heterokaryon has slight growth defects  
365 suggests that the tagged SEC-10 proteins can compete with wild type SEC-10 proteins for binding to  
366 other exocyst subunits and/or exocyst binding partners.

367 Strains expressing C-terminally tagged SEC-10-GFP at its native locus under its native promoter, or at the  
368 *his-3* locus under the *ccg-1* promoter, revealed localization of the protein at the hyphal tip. However,  
369 the endogenously tagged SEC-10-GFP strain had wider and slower growing cells and hyphal deformities  
370 including swollen hyphal tips in the homokaryotic state. The ectopically tagged SEC-10-GFP did not show  
371 an obvious phenotype, presumably because the native *sec-10* locus was intact; this strain still produces  
372 a wild type copy of SEC-10 that can assemble into functional exocyst complexes. Furthermore, our LSCM  
373 and the TEM micrographs demonstrate that a consequence of exocyst dysfunction is that the hyphae do  
374 not contain a conspicuous Spk at their apices. The phenotype observed in this strain is similar to the *sec-*  
375 *5* mutant, which displayed dispersed vesicles and irregular cell shape (Riquelme et al., 2014). Another  
376 phenotype of the C-terminally tagged SEC-10-GFP strain was a reduced interseptal distance, which  
377 meant that there were an increased number of septa throughout the length of the cell. It is possible that  
378 the disorganized Spk and accumulated vesicles at the tip correspond to vesicles that cannot be fused to  
379 the PM fast enough to turn over the input of vesicles coming from subapical regions. As more secretory  
380 vesicles are being sent to fuse to hyphal tips the vesicles accumulate in the cytoplasm and make the cells  
381 wider and swollen at the tips as they wait in queue to be processed by exocyst complexes with apparent  
382 inefficiency. This vesicle traffic jam is evidently caused by the unstable exocyst complex that cannot  
383 function optimally because the GFP molecule at SEC-10's C-terminus causes a spatial obstruction with  
384 the other exocyst subunits and/or SEC-10 binding partners. The blockage or spatial obstruction caused  
385 by the GFP molecule is enough to slow down exocytosis but not enough to block exocytosis entirely. The  
386 fact that SEC-10-GFP still localizes at the hyphal tip and that cells are still viable suggest that the exocyst  
387 is still working but is lagging in the stage between vesicle docking and vesicle fusion. The slower growth  
388 rate of the  $\Delta$ *sec-10* heterokaryon strain suggests that reduced amounts of SEC-10 protein in the cell  
389 negatively affected exocytosis and vesicle secretion. This mutant strain could not be obtained in a  
390 homokaryotic state, which confirmed that the *sec-10* gene is essential. The low production of conidia in

391 the  $\Delta sec-10$  strain could result from a dysfunctional exocyst, since the exocyst has been shown in fungi  
392 to play a role in cytokinesis and sporulation (Wang et al., 2016).

393 What could explain the dysfunction caused by C-terminally tagging SEC-10? Although the C-terminal  
394 GFP-tag appeared to disrupt SEC-10 function and incorporation into stable exocyst complexes, a  
395 deletion of the C-terminal region in the truncated mutant *sec-10*<sup>840-880del</sup> protein did not have any  
396 apparent phenotypic differences. This suggests that the predicted C-terminal disordered region of 40  
397 residues itself does not play an essential role in exocyst function. We initially hypothesized that the C-  
398 terminal end of the protein could be important to exocyst function through binding of one or more  
399 partner proteins. Upon analysis of the truncated *sec-10*<sup>840-880del</sup> mutant, however, we concluded that  
400 SEC-10 binding partners must interact with a larger region of SEC-10, or with residues located more N-  
401 terminally. Moreover, the interaction of SEC-10 to assemble into exocyst complexes does not require  
402 this C-terminal region; rather, the bulky GFP tag at the C-terminal end of SEC-10 appears to disrupt  
403 packing of SEC-10 with other subunits including SEC15 and SEC8, as observed in the *S. cerevisiae* exocyst  
404 cryo-EM structure (Mei et al).

405 Mass spectrometry analyses of the purified C-terminally tagged sample revealed that small amounts of  
406 the other seven exocyst subunits could be pulled down by SEC-10-GFP. The Mass spec analysis is  
407 sensitive and can detect proteins that the gel could not show. The number of proteins identified was  
408 only ~30% of the ones found in the GFP-SEC-10 sample. The amount of SEC-3 that co-precipitated with  
409 SEC-10-GFP was so low that it was excluded from the data after the cut-off. This finding suggests that in  
410 a C-terminally tagged SEC-10 strain, the exocyst complex is destabilized and SEC-3 does not bind tightly  
411 enough to remain bound. However, the other subunits could still bind to SEC-10, albeit with lower  
412 affinity or stability. As suggested by the phenotypic analyses, the GFP tag appears to be interfering with  
413 protein-protein interactions between SEC-10 and other subunits, leading to a more general disruption  
414 and loss of stability of the complex. Deletion of *sec-10* leads to complete disruption of the complex, but  
415 in this strain, enough complexes can assemble using the remaining wild-type protein to function in  
416 exocytosis, albeit with severe defects in growth and development.

417 SEC-10 is an essential component of the *N. crassa* exocyst complex, and it localizes at the apical dome in  
418 proximity to the plasma membrane. Deleting the *sec-10* gene from the genome is lethal and leads to a  
419 mutant phenotype in the presence of a normal copy of *sec-10*. Tagging SEC-10 at the C-terminus  
420 disrupts exocyst function when expressed in a homokaryotic state and produces a mutant phenotype.  
421 TEM reveals that the C-terminal GFP tagging causes secretory vesicles to accumulate in the cytoplasm

422 instead of in the Spk. Both the heterokaryon *sec-10* knock-out mutant and the SEC-10-GFP homokaryon  
423 have growth defects and a Spk that fails to maintain structure during polarized growth at the tip. A fully  
424 functional exocyst complex requires all eight subunits to be expressed; with the exception of SEC-5,  
425 whose knockout mutant is viable but very affected, deletion mutants for any of the other exocyst  
426 subunits are only viable if the strain is a heterokaryon expressing the wild type allele. Expressing SEC-10-  
427 GFP in all nuclei (homokaryon) produces a similar cellular phenotype as the heterokaryon  $\Delta sec-10$   
428 deletion mutant. The MS data suggests that the C-terminal tag of SEC-10 causes SEC-3 to have  
429 decreased affinity for the other exocyst subunits. Although the GFP tag is an artificial construct, its effect  
430 on exocyst function is far-reaching, and points to new roles for exocyst that warrant further  
431 investigation, including organization of macro- and microvesicles in the Spk, the frequency by which  
432 septation occurs along the cell, the continuity of membrane expansion at the tip, and maintenance of  
433 cell polarity and growth direction. The future of this work will focus on studying these pathways, as well  
434 as the role of SNAREs in exocytosis and explore how they interact with the exocyst complex, which are  
435 not fully understood in *N. crassa*. The aim will be to understand the pathways that link the exocyst and  
436 the SNARE mediated vesicle fusion.

#### 437 **Acknowledgments**

438 A. Figueroa-Meléndez was supported by CONACYT research fellowship 638116 and received a PROLAB  
439 (Promoting Research Opportunities for Latin American Biochemists program) fellowship through the  
440 American Society for Biochemistry and Molecular Biology (ASBMB). We thank the Laboratorio Nacional  
441 de Microscopía Avanzada (LNMA-CICESE), Peter Novick from the Department of Cellular and Molecular  
442 Medicine, University of California, San Diego, La Jolla, CA and The Mass Spectrometry Facility of the  
443 University of Massachusetts Medical School, Shrewsbury, MA, for technical support. We would like to  
444 thank Sam O. Obado and Peter C. Fridy from Michael Rout's lab for technical advice. This work was  
445 supported by Consejo Nacional de Ciencia y Tecnología CONACyT, Mexico, grant CB-222375 to M.R., and  
446 a grant from the National Institute of Health (GM068803) to M. M.

#### 447 **References**

448 **Dubuke, M. L. and Munson, M.** (2016). The secret life of tethers: the role of tethering factors in  
449 SNARE complex regulation. *Frontiers in Cell and Developmental Biology* **4**, 42.  
450 **Dunn, B. and Wobbe, C. R.** (1993). Preparation of protein extracts from yeast. *Current Protocols*  
451 *in Molecular Biology* **23**, 13.13. 1-13.13. 9.

452 **Fridy, P. C., Li, Y., Keegan, S., Thompson, M. K., Nudelman, I., Scheid, J. F., Oeffinger, M.,**  
453 **Nussenzweig, M. C., Fenyó, D., Chait, B. T. et al.** (2014). A robust pipeline for rapid production of  
454 versatile nanobody repertoires. *Nature Methods* **11**, 1253-1260.

455 **Friedrich, G. A., Hildebrand, J. D. and Soriano, P.** (1997). The secretory protein Sec8 is required  
456 for paraxial mesoderm formation in the mouse. *Developmental biology* **192**, 364-374.

457 **Grindstaff, K. K., Yeaman, C., Anandasabapathy, N., Hsu, S.-C., Rodriguez-Boulan, E., Scheller,**  
458 **R. H. and Nelson, W. J.** (1998). Sec6/8 complex is recruited to cell-cell contacts and specifies transport  
459 vesicle delivery to the basal-lateral membrane in epithelial cells. *Cell* **93**, 731-740.

460 **Guo, W., Grant, A. and Novick, P.** (1999). Exo84p is an exocyst protein essential for secretion.  
461 *Journal of Biological Chemistry* **274**, 23558-23564.

462 **Gupta, Y. K., Dagdas, Y. F., Martínez-Rocha, A. L., Kershaw, M. J., Littlejohn, G. R., Ryder, L. S.,**  
463 **Sklenar, J., Menke, F. and Talbot, N. J.** (2015). Septin-Dependent Assembly of the Exocyst Is Essential for  
464 Plant Infection by *Magnaporthe oryzae*. *Plant Cell* **27**, 3277-89.

465 **Heider, M. R. and Munson, M.** (2012). Exorcising the exocyst complex. *Traffic* **13**, 898-907.

466 **Honda, S. and Selker, E. U.** (2009). Tools for fungal proteomics: multifunctional *Neurospora*  
467 vectors for gene replacement, protein expression and protein purification. *Genetics* **182**, 11-23.

468 **Keller, A., Nesvizhskii, A. I., Kolker, E. and Aebersold, R.** (2002). Empirical statistical model to  
469 estimate the accuracy of peptide identifications made by MS/MS and database search. *Analytical*  
470 *chemistry* **74**, 5383-5392.

471 **Kennedy, M. J. and Ehlers, M. D.** (2011). Mechanisms and function of dendritic exocytosis.  
472 *Neuron* **69**, 856-875.

473 **Lepore, D. M., Martínez-Núñez, L. and Munson, M.** (2018). Exposing the elusive exocyst  
474 structure. *Trends in biochemical sciences* **43**, 714-725.

475 **Lopez-Franco, R., Bartnicki-Garcia, S. and Bracker, C. E.** (1994). Pulsed growth of fungal hyphal  
476 tips. *Proceedings of the National Academy of Sciences* **91**, 12228-12232.

477 **Margolin, B. S., Freitag, M. and Selker, E. U.** (1997). Improved plasmids for gene targeting at the  
478 *his-3* locus of *Neurospora crassa* by electroporation. *Fungal Genetics Newsletter*, 34-36.

479 **Martin-Urdiroz, M., Deeks, M. J., Horton, C. G., Dawe, H. R. and Jourdain, I.** (2016). The exocyst  
480 complex in health and disease. *Frontiers in Cell and Developmental Biology* **4**, 24.

481 **Mei, K., Li, Y., Wang, S., Shao, G., Wang, J., Ding, Y., Luo, G., Yue, P., Liu, J.-J. and Wang, X.**  
482 (2018). Cryo-EM structure of the exocyst complex. *Nature structural & molecular biology* **25**, 139-146.

483 **Monshausen, G. B., Messerli, M. A. and Gilroy, S.** (2008). Imaging of the Yellow Cameleon 3.6  
484 indicator reveals that elevations in cytosolic Ca<sup>2+</sup> follow oscillating increases in growth in root hairs of  
485 *Arabidopsis*. *Plant physiology* **147**, 1690-1698.

486 **Murthy, M., Garza, D., Scheller, R. H. and Schwarz, T. L.** (2003). Mutations in the exocyst  
487 component Sec5 disrupt neuronal membrane traffic, but neurotransmitter release persists. *Neuron* **37**,  
488 433-447.

489 **Murthy, M., Ranjan, R., Deneff, N., Higashi, M. E., Schupbach, T. and Schwarz, T. L.** (2005). Sec6  
490 mutations and the *Drosophila* exocyst complex. *Journal of cell science* **118**, 1139-1150.

491 **Nesvizhskii, A. I., Keller, A., Kolker, E. and Aebersold, R.** (2003). A statistical model for  
492 identifying proteins by tandem mass spectrometry. *Analytical chemistry* **75**, 4646-4658.

493 **Novick, P., Field, C., & Schekman, R.** (1980). Identification of 23 complementation groups  
494 required for post-translational events in the yeast secretory pathway. *Cell* **21**, 205-215.

495 **Picco, A., Irastorza-Azcarate, I., Specht, T., Böke, D., Pazos, I., Rivier-Cordey, A.-S., Devos, D. P.,**  
496 **Kaksonen, M. and Gallego, O.** (2017). The in vivo architecture of the exocyst provides structural basis  
497 for exocytosis. *Cell* **168**, 400-412. e18.

498 **Pogliano, J., Osborne, N., Sharp, M. D., Abanes - De Mello, A., Perez, A., Sun, Y. L. and**  
499 **Pogliano, K.** (1999). A vital stain for studying membrane dynamics in bacteria: a novel mechanism  
500 controlling septation during *Bacillus subtilis* sporulation. *Mol Microbiol* **31**, 1149-1159.  
501 **Riquelme, M., Bredeweg, E. L., Callejas-Negrete, O., Roberson, R. W., Ludwig, S., Beltran-**  
502 **Aguilar, A., Seiler, S., Novick, P. and Freitag, M.** (2014). The *Neurospora crassa* exocyst complex tethers  
503 Spitzenkörper vesicles to the apical plasma membrane during polarized growth. *Molecular biology of the*  
504 *cell* **25**, 1312-1326.  
505 **Riquelme, M., Yarden, O., Bartnicki-Garcia, S., Bowman, B., Castro-Longoria, E., Free, S. J.,**  
506 **Fleissner, A., Freitag, M., Lew, R. R., Mourino-Perez, R. et al.** (2011). Architecture and development of  
507 the *Neurospora crassa* hypha -- a model cell for polarized growth. *Fungal Biol* **115**, 446-74.  
508 **Rizzoli, S. O. and Jahn, R.** (2007). Kiss-and-run, collapse and 'readily retrievable' vesicles. *Traffic*  
509 **8**, 1137-44.  
510 **Roth, D., Guo, W. and Novick, P.** (1998). Dominant negative alleles of SEC10 reveal distinct  
511 domains involved in secretion and morphogenesis in yeast. *Molecular biology of the cell* **9**, 1725-1739.  
512 **Sánchez-León, E., Verdín, J., Freitag, M., Roberson, R. W., Bartnicki-García, S. and Riquelme,**  
513 **M.** (2011). Traffic of chitin synthase 1 (CHS-1) to the Spitzenkörper and developing septa in hyphae of  
514 *Neurospora crassa*: actin dependence and evidence of distinct microvesicle populations. *Eukaryotic Cell*  
515 **10**, 683-695.  
516 **Smith, K. M., Phatale, P. A., Sullivan, C. M., Pomraning, K. R. and Freitag, M.** (2011).  
517 Heterochromatin is required for normal distribution of *Neurospora crassa* CenH3. *Molecular and Cellular*  
518 *Biology* **31**, 2528-2542.  
519 **Strom, N. B. and Bushley, K. E.** (2016). Two genomes are better than one: history, genetics, and  
520 biotechnological applications of fungal heterokaryons. *Fungal Biology and Biotechnology* **3**, 1-14.  
521 **TerBush, D. R., Maurice, T., Roth, D. and Novick, P.** (1996). The Exocyst is a multiprotein  
522 complex required for exocytosis in *Saccharomyces cerevisiae*. *The EMBO journal* **15**, 6483.  
523 **TerBush, D. R. and Novick, P.** (1995). Sec6, Sec8, and Sec15 are components of a multisubunit  
524 complex which localizes to small bud tips in *Saccharomyces cerevisiae*. *The Journal of Cell Biology* **130**,  
525 299-312.  
526 **Verdin, J., Bartnicki-García, S. and Riquelme, M.** (2009). Functional stratification of the  
527 Spitzenkörper of *Neurospora crassa*. *Mol Microbiol* **74**, 1044-53.  
528 **Vogel, H. J.** (1956). A Convenient Growth Medium for *Neurospora crassa*. *Microbial Genetics*  
529 *Bulletin* **13**, 42-47.  
530 **Wang, N., Lee, I.-J., Rask, G. and Wu, J.-Q.** (2016). Roles of the TRAPP-II complex and the  
531 exocyst in membrane deposition during fission yeast cytokinesis. *PLoS Biology* **14**, e1002437.  
532 **Wu, B. and Guo, W.** (2015). The exocyst at a glance. *Journal of cell science* **128**, 2957-2964.  
533 **Yue, P., Zhang, Y., Mei, K., Wang, S., Lesigang, J., Zhu, Y., Dong, G. and Guo, W.** (2017). Sec3  
534 promotes the initial binary t-SNARE complex assembly and membrane fusion. *Nature communications* **8**,  
535 1-12.  
536 **Zuo, X., Guo, W. and Lipschutz, J. H.** (2009). The exocyst protein Sec10 is necessary for primary  
537 ciliogenesis and cystogenesis in vitro. *Mol Biol Cell* **20**, 2522-2529.

538

## 539 **Figure legends**

540 Figure 1. SEC-10 orthologues in other fungi have similar sizes and a conserved exocyst component  
541 sequence. Scale bar indicates amino acid residues in the sequence of the orthologues and ranges from

542 785 aa to 880 aa. Predicted domains found in SEC-10 orthologues are shown in the box legend; the size  
543 of the domain represents the actual scale of the sequence.

544 Figure 2. Laser scanning confocal microscopy of *N. crassa* hyphae expressing SEC-10-GFP and GFP-SEC-  
545 10 reveal that SEC-10 protein is localized at the hyphal tip in the apical dome: A) Under control of native  
546 promoter and in a heterokaryotic state, and B) Under control of *Pccg-1* expressed ectopically from the  
547 *his-3* locus. C) Time lapse of growing hypha that expresses SEC-10-GFP in a heterokaryotic state. D) Time  
548 lapse of SEC-10-GFP expressed in a homokaryotic state. E) Time lapse N-terminal GFP-SEC-10 expressed  
549 in a homokaryotic state. Scale bars = 10  $\mu$ m.

550 Figure 3. DIC and LSCM of SEC-10-GFP homokaryon strains show hyphae that are hyperseptated and  
551 swollen at the tips. A) FM4-64 staining of the SEC-10-GFP strain shows that FM4-64 stained the plasma  
552 membrane surrounding the cytoplasm, the septa and the accumulated at the apex in a disperse cloud.  
553 B) Differential interference contrast (DIC) microscopy of a hypha of the SEC-10-GFP homokaryon strain.  
554 Under DIC the hypha revealed an unusual pattern of subapical septa (white arrows). In contrast, C) FM4-  
555 64 staining of a wild-type strain showing the stained plasma membrane and the Spk (white arrow) with  
556 an unstained core (top image). DIC microscopy of the same hypha displayed above (bottom image).  
557 Scale bars = 10  $\mu$ m.

558 Figure 4. Qualitative comparison of the growth and morphology of the strains expressing SEC-10-GFP  
559 heterokaryon and homokaryon and the wild-type strain 9718. A) Phenotype of the different strains of *N.*  
560 *crassa* grown on MMV plates and incubated for 24 hours and for one week at 30 ° C. B) Morphology of  
561 the edge of the colonies viewed by stereomicroscopy. C) Differential interference contrast (DIC)  
562 microscopy of hyphae observed with a 60X objective. Scale bars B = 2mm and 200  $\mu$ m, C = 10  $\mu$ m

563 Figure 5. Effect of the expression of SEC-10-GFP in a heterokaryon strain on Spk organization and growth  
564 revealed by time-lapse microscopy. Spk was stained with FM4-64 and observed by Laser scanning  
565 confocal microscopy. SEC-10-GFP heterokaryons have minor irregularities in cell shape, as seen in the  
566 white dotted outline of the cells. The fluorescence of the Spk is lost as growth pauses and reappears  
567 when growth resumes. The position of the FM4-64 stained Spk changes with the corresponding changes  
568 in growth direction (white arrows). Scale bar = 10  $\mu$ m.

569 Figure 6. Tagging SEC-10 with GFP at its C-terminus disrupts growth in homokaryons, and the *sec-10*  
570 knock out mutation is lethal and dominant in heterokaryons. A) Schematic view of the DNA constructs  
571 used. DNA constructs were incorporated into endogenous loci via electroporation and the strains were  
572 selected by hygromycin resistance (*hph*). B) Left column shows colony growth of the strains after 24  
573 hours. Laser scanning confocal microscopy of strains stained with FM4-64 reveal vesicle distribution  
574 inside the cell. The DIC microscopy shows the difference in morphology between the different strains.  
575 The right column chart shows growth rate of the strains: wild type (orange), GFP tagged (green), and  
576 *sec-10* mutants (blue). Scale bar = 10  $\mu$ m.

577 Figure 7. TEM micrographs of hyphal tips of *N. crassa* SEC-10-GFP homokaryon strain (A-B). Tips lacked  
578 the characteristic outer layer of macrovesicles and inner layer of microvesicles seen in the Spk.  
579 Macrovesicles are seen dispersed in the cytoplasm (arrowheads in A). The SPK core could be clearly seen

580 but lacking an outer core (A) with microvesicles present (arrows in B), while in others a core could not be  
581 clearly visualized (C). C.1 and C.2 are magnifications of the dotted line 1 and 2 regions in C. Scale bars A =  
582 2  $\mu\text{m}$ , B = 200 nm, C = 5  $\mu\text{m}$ , C.1 = 1  $\mu\text{m}$ , C.2 = 1  $\mu\text{m}$ .

583 Figure 8. LSCM analysis of strains co-expressing SEC-10-GFP and vesicular markers CHS-1-mChFP or GS-  
584 1-mChFP. A) Localization of CHS-1-mChFP in the Spk core. The overlapping signals emitted by GFP and  
585 by mChFP reveal that SEC-10-GFP does not co-localize with microvesicles. B) GS-1-mChFP localizes at the  
586 outer Spk layer seen as a donut shaped apical body. The overlapping of the signals emitted by GFP and  
587 by mChFP reveal partial colocalization. SEC-10 and GS-1 partially colocalize as seen in the fluorescence  
588 intensity profile in 2  $\mu\text{m}$  distance from the tip. The white line is the distance analyzed in graph. Scale  
589 bars = 10  $\mu\text{m}$ .

590 Figure 9. SDS-PAGE and Krypton staining of purified *N. crassa* proteins pulled down by Lag94-15  
591 magnetic beads and unique peptides identified by mass spectrometry. A) The first lane of the stained gel  
592 shows cytoplasmic GFP pull-down from a GFP producing strain. Second lane reveals a thick band of SEC-  
593 10-GFP and possibly other subunits such as SEC-8 and/or SEC-5. Third lane shows the intact exocyst pull-  
594 down by GFP-SEC-10 and Lag94-15. B) Venn diagram depicting the number of proteins detected by mass  
595 spectrometry analysis. The left circle of the diagram shows the number of unique proteins identified  
596 from the C-terminally tagged sample, the right section corresponds to the N-terminally tagged sample  
597 and the intersection contains the proteins shared between both. C) Bar graph comparing the results  
598 between the two samples. The X axis shows the number of hits for each of the exocyst subunits while  
599 the Y axis shows the unique proteins identified in the N-terminally tagged sample and the C-terminally  
600 tagged sample. The subunits are color coded and are placed in the graph in the same order as the key  
601 legend.

## 602 **Supplementary Videos**

603 Supplementary Video 1. DIC video capture coupled with LSCM of SEC-10-GFP homokaryon strains  
604 stained with FM4-64.

605 Supplementary Video 2. LSCM video capture of the SEC-10-GFP strain showing the characteristic paused  
606 growth and moving Spk revealed by FM4-64 staining.

607 Supplementary Video 3. LSCM video capture of the GFP-SEC-10 strain stained with FM4-64.

## 608 **Supplementary Figures**

609 Supplementary Figure S1. Schematic representation of the methodology used to generate replacement  
610 DNA constructs. DNA templates are labeled by gene name and its adjacent UTR whether it is at the 5' or  
611 3' end. The PCR products are shown with their respective primers and overhangs. A) C-terminal tagging  
612 of SEC-10 using *sec-10::10XGly::gfp::hph* and *hph::3' UTR* cassettes. B) N-terminal tagging of SEC-10 using  
613 a *Pccg::N-gfp* fragment that was fused to *hph* and *sec-10* fragments. C) Eliminating *sec-10* by UTR  
614 targeting replacement cassettes. D) Eliminating 40 amino acids from the C-terminus of SEC-10 by *hph*  
615 selectable gene replacement cassettes that excludes 120 nucleotides in the sequence (red box).

616 Supplementary Figure S2. One-way ANOVA analysis of hyphal diameters between the different *N. crassa*  
 617 strains. The strains displayed on the chart from left to right are the 9718 wild type strain, the SEC-10-  
 618 GFP homokaryon strain (C-terminal tag) and the GFP-SEC-10 homokaryon strain (N-terminal tag). The  
 619 SEC-10-GFP homokaryon strain had significantly wider cells, compared to the other two strains.

620 Supplementary Figure S3. Bar graph displaying the total peptides identified in the samples and their  
 621 Gene Ontology (GO) Categories. A) The X axis shows the number of hits for each of the proteins  
 622 identified in the samples whereas the Y axis shows the name of the proteins identified in both the GFP-  
 623 SEC-10 and SEC-10-GFP sample. B-D) The X axis represents the number of different proteins classified  
 624 under the same GO term and the Y axis shows the name of the GO term. The red colored bars are  
 625 proteins found in the N-terminally tagged sample and the blue color bars are proteins found in the C-  
 626 terminally tagged sample.

627

628

629

### 630 Supplementary Tables

631 Supplementary Table 1. Strains used or generated in this study.

Strain number	Genotype	Source
<b>N1</b>	<i>mat a</i> ; WT	FGSC988
<b>N150</b>	<i>mat A</i> ; WT	FGSC9013
<b>SMRP24</b>	<i>mat A</i> ; $\Delta$ <i>mus-51::bar+</i> ; <i>his-3</i>	FGSC9717
<b>SMRP25</b>	<i>mat a</i> ; $\Delta$ <i>mus-51::bar+</i>	FGSC9718
<b>SMRP90</b>	<i>mat A</i> ; <i>Pccg-1::chs-1::chfp</i>	Verdin et al., 2009
<b>SMRP93</b>	<i>mat A</i> ; <i>Pccg-1::gs-1::chfp</i>	Verdin et al., 2009
<b>SMRP410</b>	<i>mat A</i> ; <i>Pccg-1::sec-10::gfp</i> Heterokaryon	This study
<b>SMRP411</b>	<i>mat a</i> ; <i>Psec-10::sec-10::10xGly::gfp::loxp::hph::loxp</i> ; $\Delta$ <i>mus-51::bar<sup>+</sup></i> Heterokaryon	This study
<b>SMRP412</b>	<i>mat a</i> ; <i>Psec-10::sec-10::10xGly::gfp::loxp::hph::loxp</i> ; $\Delta$ <i>mus-51::bar<sup>+</sup></i> Homokaryon	This study
<b>SMRP487</b>	<i>mat a</i> ; $\Delta$ <i>mus-51::bar<sup>+</sup></i> ; <i>sec-10<sup>2523_2640del</sup>::hph<sup>+</sup></i> Homokaryon	This study
<b>SMRP488</b>	<i>mat a</i> ; $\Delta$ <i>sec-10::hph<sup>+</sup></i> ; $\Delta$ <i>mus-51::bar<sup>+</sup></i> Heterokaryon	This study
<b>SMRP489</b>	<i>mat a</i> ; <i>hph<sup>+</sup>::Pccg-1::gfp::sec-10</i> ; $\Delta$ <i>mus-51::bar<sup>+</sup></i> Homokaryon	This study

632

633 Supplementary Table 2. Oligonucleotides used in this study.

Laboratory number	Name	5' – 3' Sequence
<b>260</b>	hph SM-R	TCGCCTCGCTCCAGTCAATGACC
<b>261</b>	hph SM-F	AAAAAGCCTGAACTCACCGGACG
<b>298</b>	loxP-R	CGAGCTCGGATCCATAACTTCGTATAGCA
<b>299</b>	10xGly-F	GGCGGAGGCGGCGGAGGCGGAGGCGGAGG

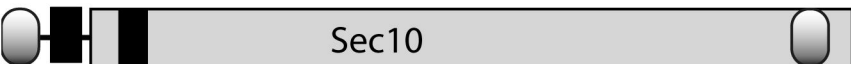
<b>421</b>	sec10GlyF	CGATTCGTCAGACCTTACGCCAC
<b>422</b>	sec10loxF	TGCTATACGAAGTTATGGATCCGAGCTCGAAGATATTGCGAGTTTTGGTGGGG
<b>423</b>	sec10loxR	GGTCTGGGTCTGGGTTTGC GACTG
<b>724</b>	orf sec10 R	CTCGTCAACAAGAGATTGCAGACTG
<b>725</b>	gfp 8xGly R	GCCGCCTCCGCCCTCCGCCCTTGTACAGCTCGTCCATG

---

634

200 400 600 800 1000

SEC-10 880 aa *Neurospora crassa*



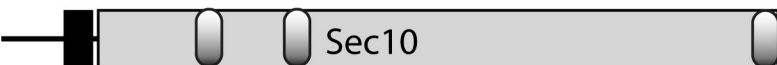
SEC-10 871 aa *Saccharomyces cerevisiae*



SEC-10 851 aa *Magnaporthe oryzae*



SEC-10 813 aa *Aspergillus nidulans*



SEC-10 785 aa *Candida albicans*

